Inorganic Chemistry Research

Article

New Copper(II) Complexes with Benzimidazole and Benzoxazole Heterocyclic Ligands: Synthesis, Spectral Characterization, FMO, MEP, NBO, and DFT Study

Hadi Kargar[a,*], Mehdi Fallah-Mehrjardi[b], Reza Behjatmanesh-Ardakani[b], Khurram Shahzad Munawar[c,d]

[a]*Department of Chemical Engineering, Faculty of Engineering, Ardakan University, P.O. Box 184, Ardakan, Iran*
[b]*Department of Chemistry, Payame Noor University (PNU), 19395-4697, Tehran, Iran*
[c]*Department of Chemistry, University of Sargodha, Punjab, Pakistan*
[d]*Department of Chemistry, University of Mianwali, Mianwali, Pakistan*

Received: February 1, 2022; Accepted: March 17, 2022
Cite This: *Inorg. Chem. Res.* **2022**, *6*, 48-57. DOI: 10.22036/icr.2022.327584.1124

Abstract: 3-Ethoxy salicylaldehyde on reaction with 1,2-phenylenediamine and 2-aminophenol yielded heterocyclic ligands (**HL^{BIZ}** and **HL^{BOZ}**) under ultrasonic irradiation in ethanol solvent. The reaction of these ligands with copper(II) acetate monohydrate salt led to the related **Cu(L)$_2$** complexes in methanol solvent. FT-IR, ^{1}H & ^{13}C NMR, and elemental analysis were used to investigate the structures of the synthesized ligands, while the copper(II) complexes were characterized by CHN analysis and FT-IR spectroscopy. The imino nitrogens and phenolic oxygens are involved in the coordination of the ligands to the Cu^{2+} ions to generate the complex. The parameters estimated by DFT at the B3LYP/Def2-TZVP level of theory show that the theoretical values are consistent with the experimental findings.

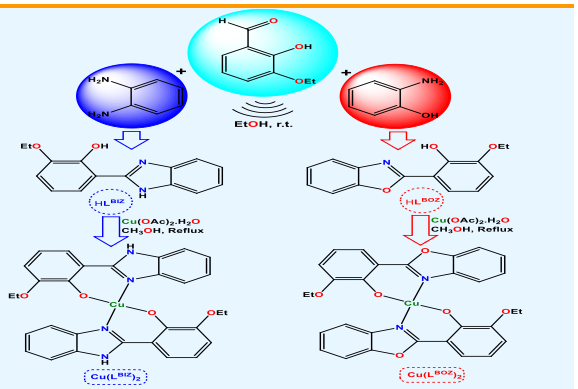

Keywords: Heterocyclic ligand, Benzimidazole, Benzoxazole, Copper(II) complex, DFT

1. INTRODUCTION

In today's world, heterocyclic compounds are being evaluated as unique products with an extensive variety of biological, agronomic, medical, industrial, and other applications.[1] The nitrogen donor ligands constitute a very fascinating area of research because they have a proclivity for complexing with various transition metals and are well-known pharmacophores for drug development.[2]

The benzimidazole (BIZ) moiety is a bicyclic molecule containing a benzene ring fused with an imidazole scaffold.[3] Benzimidazole and its derivatives are heterocyclic compounds and have a wide spectrum of biological applications due to structural relevance with common nucleobases.[4-11] In addition to their biological importance, benzimidazoles are equally important in the arena of the chemistry of coordination compounds. The derivatives of benzimidazole are very strong chelating agents and can form stable metal complexes with a variety of transition metals.[12-14] Many groups have discovered that benzimidazole-based metal complexes have a wide range of structural diversity, including mononuclear and multinuclear, and ring-like coordination compounds.[15-18] The copper(II) complexes with benzimidazole are potentially active against several bacterial and fungal species and can bind to DNA and also have cytotoxic potential against tumor cells.[19-23] In addition to this, benzimidazole-based-copper complexes show solid-state fluorescent properties, exhibit in vitro antidiabetic potential, and can inhibit α-amylase.[24]

Benzoxazole (BOZ), a planar heterocyclic molecule composed of a benzene ring fused with an oxazole ring, is a very well-known compound and is frequently used as a precursor for the industrial preparation of various pharmacological drugs.[25] These are important biomolecules that have a wide range of biological and pharmacological properties.[26-29] They also have unique properties, including simplicity of preparation, electrochemical behaviour, visible light absorption, structural flexibility, supramolecular architecture, long-lived electrically excited states, and luminescence.[30-32] The benzoxazole derivatives and their complexes with metals, especially copper, have also been extensively studied as chelating agents *via* nitrogen atoms for the synthesis of metal complexes of biological, industrial, spectral luminescent, cytotoxic, and antiproliferative properties.[33-35]

Therefore, on the basis of the applications of heterocyclic compounds, and concerning our research on transition

metal complexes,[36-45] we opted to synthesize copper(II) complexes with heterocyclic ligands (benzimidazole and benzoxazole). The main objectives of the current study are the synthesis and characterization of the synthesized ligands and complexes, and theoretical studies like FMO, MEP, and NBO analysis of the synthesized compounds by DFT at the B3LYP/Def2-TZVP level of theory.

2. EXPERIMENTAL

Materials and Methods

All chemical materials, reagents, and solvents applied in the present studies are of analytical grade and purchased from Merck, Acros Organics, Sigma-Aldrich, and Alfa Aesar. The %age composition of C, H, and N was evaluated using a Leco CHNS elemental analyzer. The ^{1}H NMR spectral studies were carried out with the use of a BRUKER AVANCE 400 MHz spectrometer. The chemical shift values (δ) are provided by correlating them to an internal standard reference tetramethylsilane (TMS). The IRPrestige-21 Spectrophotometer was used to run infrared spectra to validate various functional groups contained in the manufactured compounds by following the KBr discs method. The sonication of the reaction mixture was performed using a UP 400S ultrasonic processor with a 3 mm broad and 140 mm long probe that was submerged precisely in the reaction mixture. The reactions were performed under the influence of ultrasonic irradiation in a 40 cm^3 reactor made up of glass at room temperature.

Syntheses

Syntheses of heterocyclic ligands (HL^{BIZ} and HL^{BOZ}). 10 mmol of 3-ethoxy salicylaldehyde was mixed to an ethanolic solution (25 mL) of 1,2-phenylenediamine or 2-aminophenol (10 mmol). The solution was irradiated with ultrasonic waves at room temperature for a suitable amount of time (5 min for the HL^{BIZ} and 10 min for HL^{BOZ}) till the reaction was accomplished, as confirmed by TLC (eluent, n-hexane:ethyl acetate, 5:2). The reaction mixture was then filtered, and the products were recrystallized, afterward, from the EtOH to obtain the targeted compounds with the maximum possible purity. The ultrasonic wave-assisted method is preferred over the conventional reflux method because it completes the reaction not only at room temperature but also takes a very short time.

HL^{BIZ}: Yield 89%. Anal. Calc. for $C_{15}H_{14}N_2O_2$: C, 70.85; H, 5.55; N, 11.02, Found: C, 70.98; H, 5.58; N, 10.93 %. FT-IR (KBr, cm^{-1}); 3437 (υ_{N-H}); 1622 ($\upsilon_{C=N}$); 1547, 1479 ($\upsilon_{C=C}$); 1249 (υ_{C-O}). ^{1}H NMR (400 MHz, $CDCl_3$, ppm): 1.51 [t, 3 H, -CH_3, ^3J = 7.0 Hz], 4.15 [q, 2 H, -OCH_2, ^3J = 7.0 Hz], 6.77-7.12 [m, 7 H, Aromatic-H], 8.63 [s, 1 H, -NH], 13.52 [s, 1 H, -OH]. ^{13}C NMR (100 MHz, $CDCl_3$, ppm): 14.9, 64.5, 115.8, 118.2, 118.7, 118.8, 119.5, 123.7, 128.2, 134.8, 141.0, 147.6, 151.0, 161.9, 164.4 [46].

HL^{BOZ}: Yield 83%. Anal. Calc. for $C_{15}H_{14}NO_3$: C, 70.58; H, 5.13; N, 5.49, Found: C, 70.77; H, 5.11; N, 5.62 %. FT-IR (KBr, cm^{-1}); 1628 ($\upsilon_{C=N}$); 1543, 1469 ($\upsilon_{C=C}$); 1277 (υ_{C-O}). ^{1}H NMR (400 MHz, $CDCl_3$, ppm): 1.51 [t, 3 H, -CH_3, ^3J = 7.0 Hz], 4.15 [q, 2 H, -OCH_2, ^3J = 7.0 Hz], 6.89-7.24 [m, 7 H, Aromatic-H], 12.54 [s, 1 H, -OH]. ^{13}C NMR (100 MHz, $CDCl_3$, ppm): 14.9, 64.6, 115.9, 116.4, 118.1, 119.1, 119.4, 121.0, 123.9, 128.8, 135.4, 147.6, 150.1, 150.8, 163.3.

Syntheses of $Cu(L)_2$ complexes. To a solution of 1 mmol (0.200 g) of $Cu(CH_3COO)_2.H_2O$ in 50 mL of MeOH has been added a solution of either HL^{BIZ} or HL^{BOZ} (2 mmol) dissolved in 5 mL of hot MeOH. The resulting solution was held at reflux for 1 hour to get the precipitates of desired products, which were then filtered out and washed separately, using equal parts of H_2O and MeOH.

$Cu(L^{BIZ})_2$: Yield 71%. Anal. Calc. for $C_{30}H_{26}CuN_4O_4$: C, 63.20; H, 4.60; N, 9.83, Found: C, 63.52; H, 4.63; N, 9.71 %. FT-IR (KBr, cm^{-1}); 3423 (υ_{N-H}); 1601 ($\upsilon_{C=N}$); 1579, 1491 ($\upsilon_{C=C}$); 1294 (υ_{C-O}), 545 (υ_{Cu-O}), 470 (υ_{Cu-N}).

$Cu(L^{BOZ})_2$: Yield 67%. Anal. Calc. for $C_{30}H_{24}CuN_2O_6$: C, 62.99; H, 4.23; N, 11.11, Found: C, 63.27; H, 4.20; N, 11.23 %. FT-IR (KBr, cm^{-1}); 1605 ($\upsilon_{C=N}$); 1539, 1481 ($\upsilon_{C=C}$); 1319 (υ_{C-O}), 536 (υ_{Cu-O}), 424 (υ_{Cu-N}).

Computational details

All DFT calculations were performed utilizing the Gaussian code,[47] the B3LYP hybrid method,[48] and the Def2-TZVP basis set.[49] To model the solution phase, the integral equation formalism variant of the PCM (IEFPCM) approach was used to include solute-solvent interactions.[50] In this method, the solute cavity is created by a set of overlapping spheres. After optimization, the frequency analysis was performed to ensure that the structure corresponds to a minimum on the potential energy surface (PES) of the molecule. The Gauge-Independent Atomic Orbital (GIAO) technique [51] was utilized to calculate NMR data. Chemical shifts (δ) of the H_2L ligands were performed at B3LYP/Def2-TZVP in $CDCl_3$. The values of chemical shifts (δ) were calculated by subtracting the appropriate isotropic portion of the shielding tensor from tetramethylsilane $\delta i = \sigma_{TMS} - \sigma i$. The B3LYP/Def2-TZVP level of theory established the solution phase isotropic shielding constants for tetramethylsilane to be 184.52 ppm for the ^{13}C and 31.92 ppm for the ^{1}H nuclei. The Chemissian software[52] was used to create contour plots of the lowest unoccupied molecular orbital (LUMO) and the highest occupied molecular orbital (HOMO). Molecular electrostatic potential (MEP) data was computed by Gaussian/GaussView programs. The natural bond orbital (NBO) calculations were performed with the help of the NBO 6.0 program.[53]

3. RESULTS AND DISCUSSION

Syntheses

Heterocyclic ligands (HL^{BIZ} and HL^{BOZ}) were produced through the reaction of 3-ethoxy salicylaldehyde with 1,2-phenylenediamine and 2-aminophenol, respectively, under ultrasonic irradiation in ethanol (Scheme 1). The reaction of copper(II) acetate monohydrate with these ligands in methanol led to the $Cu(L)_2$ complexes (Scheme 2).

FT-IR spectra

FT-IR spectra of the ligands and their corresponding Cu(II) complexes are presented in Figures 1 and 2. The important coordination sites of the ligands which are getting involved in chelation were identified by comparing their FT-IR spectra with those of complexes. Important stretching vibrational bands of -C=N were

noticed at 1622 and 1628 cm^{-1} for heterocyclic ligands.[54] In the complexes, these bands are shifted to a lower frequency (1601 and 1605 cm^{-1}). The decrease in the double bond character of the -C=N band generated by the coordination of nitrogen atoms to the metal centers causes these alterations, which are consistent with the results obtained from structurally similar compounds documented earlier.[55] Because of oxygen atom's participation in coordination, the positions of C–O stretching vibrational bands in the free form of ligands (1249 and 1277 cm^{-1}) shift towards higher frequency regions on complexation (1294 and 1319 cm^{-1}).[56] The emergence of faint bands at low wavenumbers that were ascribed to Cu-O and Cu-N also indicated the coordination of nitrogen and oxygen atoms.[57]

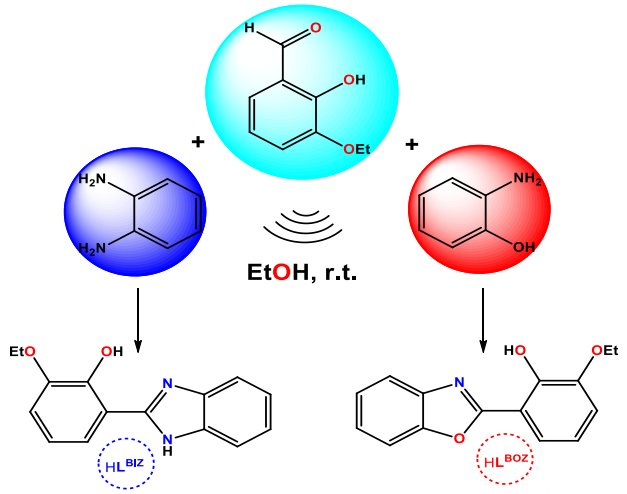

Scheme 1. Syntheses of heterocyclic ligands (**HL^{BIZ}** and **HL^{BOZ}**) under ultrasonic irradiation

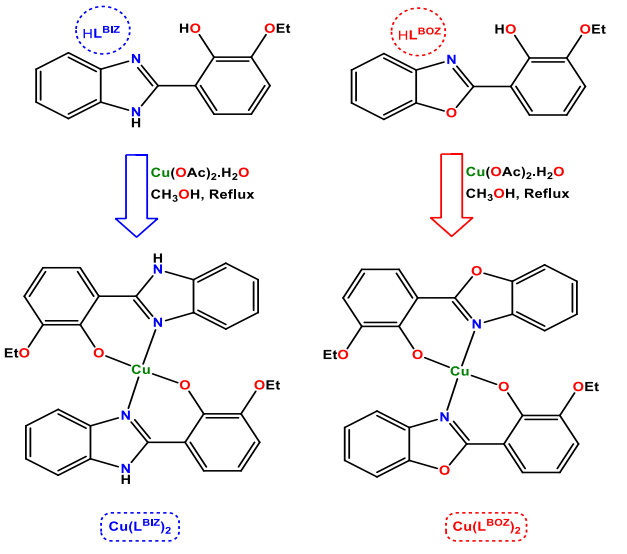

Scheme 2. Syntheses of copper(II) complexes **[Cu(L^{BIZ})$_2$** and **Cu(L^{BOZ})$_2$]**

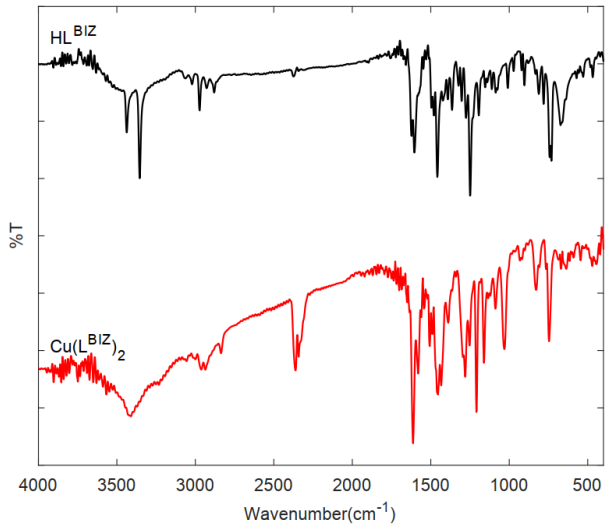

Figure 1. The experimental FT-IR stacked spectrum of the **HL^{BIZ}** ligand and **Cu(L^{BIZ})$_2$** complex.

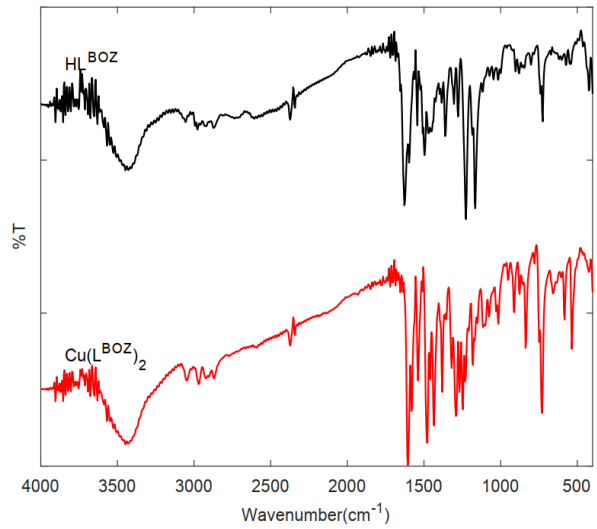

Figure 2. The experimental FT-IR stacked spectrum of the **HL^{BOZ}** ligand and **Cu(L^{BOZ})$_2$** complex.

The gas-phase spectra of the synthesized compounds calculated by the B3LYP/Def2-TZVP level of theory are given in Figures 3 and 4. The high similarity of experimental and theoretical spectra indicates that the structures of the synthesized compounds are close to each other in solid and gas phases. Experimental and theoretical vibrational frequencies along with relative errors for the ligands and their complexes are given in Table 1. To get the corrected values that are closer to the experimental values, the calculated frequencies were multiplied by a scaling factor of 0.965.[58] The highest percentage difference between the two types of results is 2.43, which is due to the use of the harmonic approximation for vacuum computations.

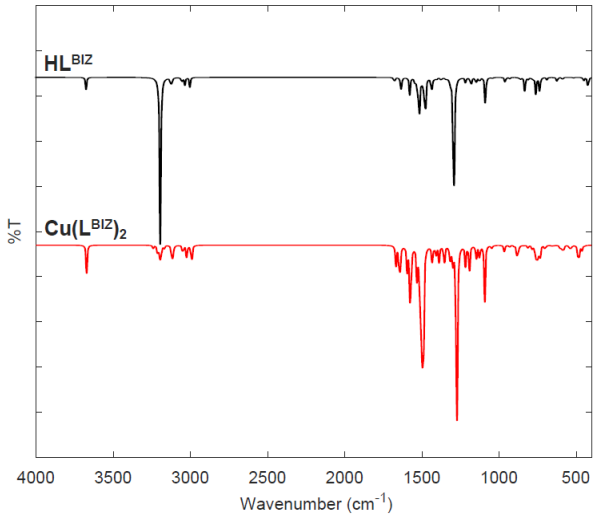

Figure 3. The theoretical FT-IR stacked spectrum of the **HL^{BIZ}** ligand and **Cu(L^{BIZ})$_2$** complex.

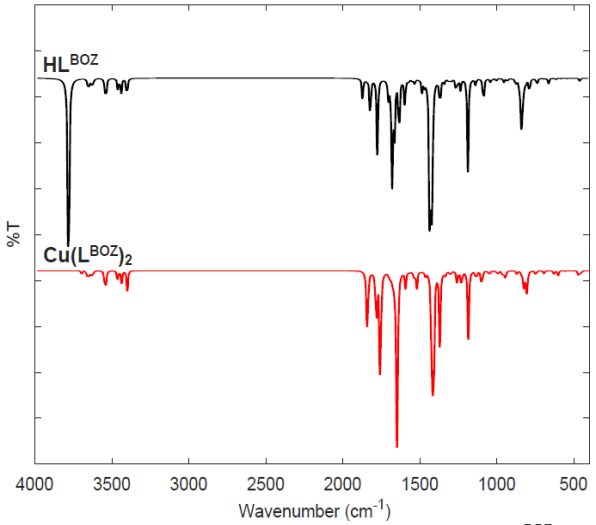

Figure 4. The theoretical FT-IR stacked spectrum of the **HL^{BOZ}** ligand and **Cu(L^{BOZ})$_2$** complex.

Table 1. The experimental and calculated infrared vibrational parameters (cm^{-1}) along with relative errors of the heterocyclic ligands and their corresponding copper(II) complexes

Assignment		ν(C=N)	ν(C–O)	ν(Cu–O)	ν(Cu–N)
HL^{BIZ}	Experimental	1622	1249	-	-
	Calculated	1609	1241	-	-
	Relative error (%)[a]	-0.80	-0.64	-	-
HL^{BOZ}	Experimental	1628	1277	-	-
	Calculated	1606	1283	-	-
	Relative error (%)	-1.35	0.47	-	-
Cu(L^{BIZ})$_2$	Experimental	1601	1294	545	470
	Calculated	1604	1300	552	459
	Relative error (%)	0.19	0.46	1.28	-2.34
Cu(L^{BOZ})$_2$	Experimental	1605	1319	536	424
	Calculated	1591	1318	549	420
	Relative error (%)	-0.87	-0.08	2.43	-0.94

[a]Relative error (%) = $(X^{Calc} - X^{Exp})*100/X^{Exp}$.

NMR spectra

^1H & ^{13}C NMR spectra of the heterocyclic ligands were recorded in deuterated chloroform ($CDCl_3$). ^1H NMR spectral details of the ligands are specified in the experimental part and the spectra are manifested in Figures 5 and 6. The important peaks in the proton NMR spectra of the **HL^{BIZ}** and **HL^{BOZ}** appear at δ = 13.52 and 12.54 ppm respectively is attributed to the phenolic protons of ligands. All aromatic protons in the ligands show their presence in the projected regions from δ = 6.77 to 7.24 ppm. The signals for aliphatic protons in the ligands show their presence in the projected regions from δ = 1.51 to 4.15 ppm.

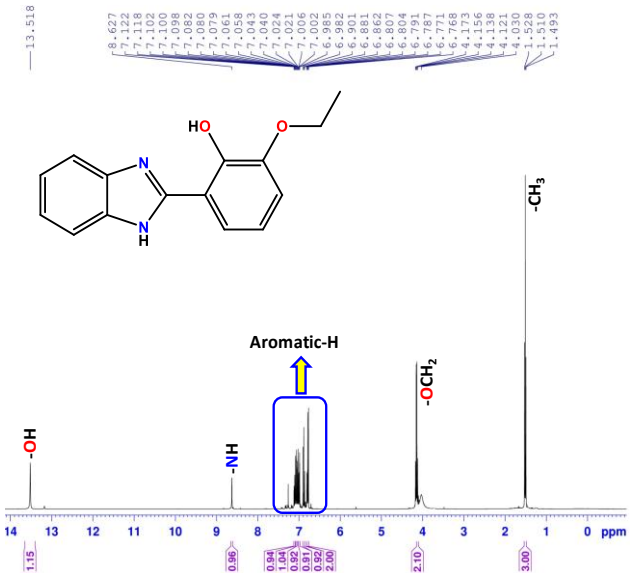

Figure 5. ^1H NMR spectrum of the **HL^{BIZ}** ligand in $CDCl_3$.

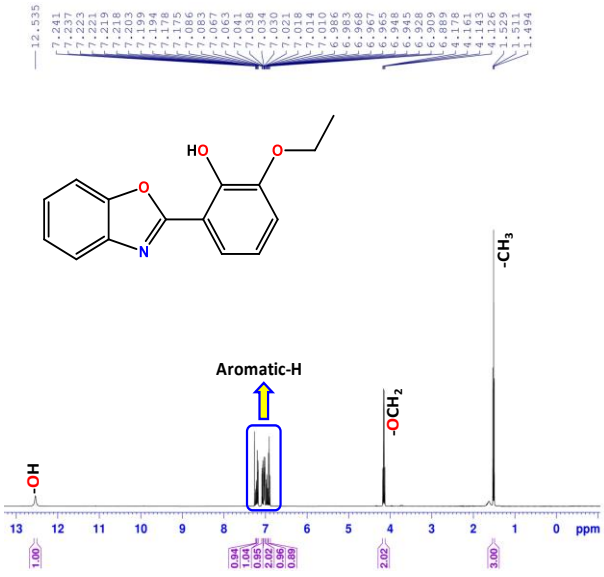

Figure 6. ^1H NMR spectrum of the **HL^{BOZ}** ligand in $CDCl_3$.

The ^{13}C NMR spectra of the heterocyclic ligands are shown in Figures 7 and 8. The signals for the methine carbon in the spectra of the **HL^{BIZ}** and **HL^{BOZ}** are observed at δ = 164.4 and 163.3, respectively and the signals for the phenolic carbon in the spectra of these ligands are visible at δ = 161.9 and 150.8, respectively. The other aromatic and aliphatic carbons of the ligands are appeared in their respective regions according to the literature.[59] The experimentally observed and computationally calculated NMR data of the heterocyclic ligands are compatible with each other (Tables 2 and 3).

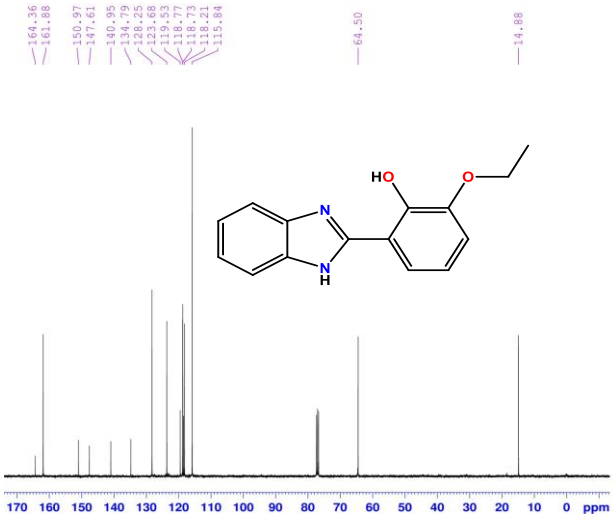

Figure 7. ^{13}C NMR spectrum of the **HL^{BIZ}** ligand in $CDCl_3$.

DFT optimized structures

In order to investigate the geometries of the synthesized ligands and their Cu(II) complexes, their structures were optimized to locate the local minimum at B3LYP/Def2-

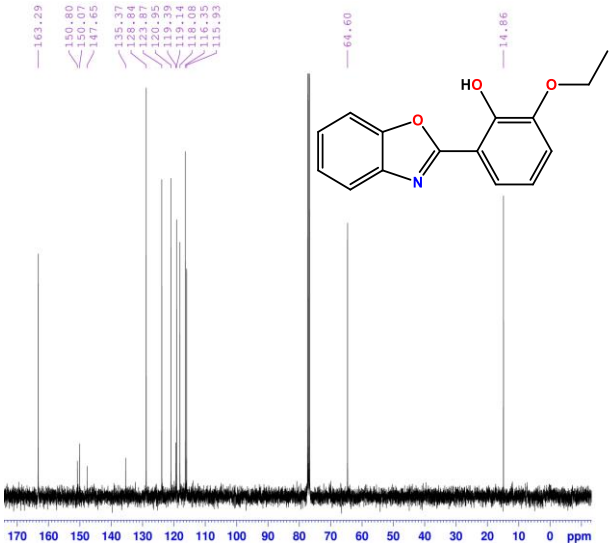

Figure 8. ^{13}C NMR spectrum of the **HL^{BOZ}** ligand in $CDCl_3$.

TZVP level of theory. Figure 9 shows the gas phase optimized structures of the heterocyclic ligands and their copper(II) complexes. Also, Table 4 lists the computed findings, including bond lengths and bond angles, for **Cu(L^{BIZ})$_2$** and **Cu(L^{BOZ})$_2$** complexes, which exhibit the distorted square planar geometry for both complexes.[60-62] The **Cu(L^{BIZ})$_2$** and **Cu(L^{BOZ})$_2$** complexes can have two geometric stereoisomers, *cis* and *trans* (Figure 10). The sum of the electronic and the zero-point energy (E^{ZPE}), enthalpy (H), and Gibbs free energy (G) of both *cis* and *trans* isomers of the complexes are reported in Table 5. Data show that *trans* isomers are more stable in both complexes (~5 kcal mol^{-1} for **Cu(L^{BIZ})$_2$** and ~6 kcal mol^{-1} for **Cu(L^{BOZ})$_2$**).[60-62]

Table 2. Experimental and calculated chemical shift values (ppm) in ^1H NMR spectra of the heterocyclic ligands[a]

	-CH_3	-OCH_2	Aromatic-H	-NH	-OH
+HL^{BIZ}	1.51 (1.53)	4.15 (4.06)	6.77-7.12 (7.10-8.01)	8.63 (9.18)	13.52 (13.76)
HL^{BOZ}	1.51 (1.54)	4.15 (4.08)	6.89-7.24 (7.19-8.01)	-	12.54 (12.18)

[a]The calculated ^1H NMR chemical shifts are reported in parenthesis.

Table 3. Experimental and calculated chemical shift values (ppm) in ^{13}C NMR spectra of the heterocyclic ligands[a]

	-C=N	-C-OH	-C-OEt	Aromatic-C	-CH_2	-CH_3
HL^{BIZ}	164.4 (160.2)	161.9 (159.5)	151.0 (158.1)	115.8-147.6 (115.1-149.9)	64.5 (69.5)	14.9 (17.4)
HL^{BOZ}	163.3 (173.2)	150.8 (160.0)	150.1 (158.0)	115.9-147.6 (115.8-157.3)	64.6 (69.6)	14.9 (17.4)

[a]The calculated ^{13}C NMR chemical shifts are reported in parenthesis.

Table 4. Selected theoretical bond lengths (Å) and bond angles (°) in **Cu(L^{BIZ})$_2$** and **Cu(L^{BOZ})$_2$** complexes

Bond lengths	**Cu(L^{BIZ})$_2$**	**Cu(L^{BOZ})$_2$**	Bond angles	**Cu(L^{BIZ})$_2$**	**Cu(L^{BOZ})$_2$**
Cu1-O1	1.920	1.915	N1-Cu1-O1	90.75	90.98
Cu1-N1	2.004	2.010	N1-Cu1-O1^i	93.39	93.73
O1-C1	1.296	1.295	N1-Cu1-N1^i	158.05	156.83
O2-C2	1.358	1.359	N1^i-Cu1-O1	93.39	93.73
N1-C7	1.333	1.318	N1^i-Cu1-O1^i	90.73	90.98
N2 (or O3)-C7	1.369	1.362	O1^i-Cu1-O1	158.17	156.41

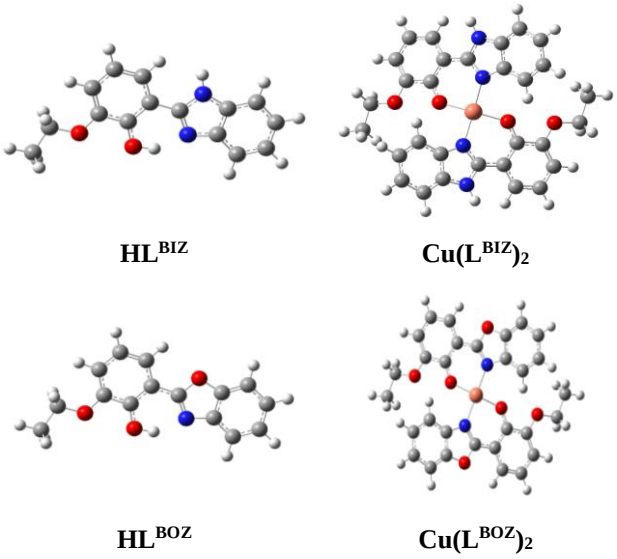

Figure 9. DFT optimized geometries of heterocyclic ligands and their copper(II) complexes at B3LYP/Def2-TZVP.

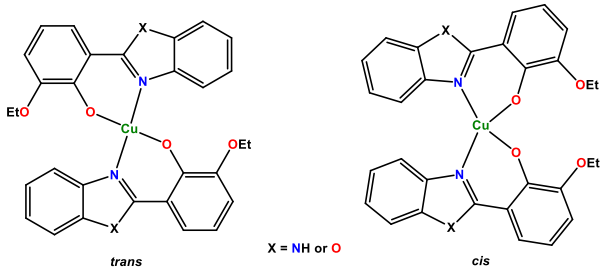

Figure 10. Two possible geometric stereoisomers for **Cu(L^{BIZ})$_2$** and **Cu(L^{BOZ})$_2$** complexes.

Table 5. Sum of the electronic and the zero-point energy (E^{ZPE}), enthalpy (H), and Gibbs free energy (G) of the complexes. All values are in Hartree unit

	Cu(L^{BIZ})$_2$		Cu(L^{BOZ})$_2$	
	cis	***trans***	***cis***	***trans***
E^{ZPE}	-3319.555	-3319.564	-3359.310	-3359.320
H	-3319.521	-3319.529	-3359.276	-3359.286
G	-3319.624	-3319.632	-3359.378	-3359.388

1 Hartree = 627.5095 kcal.mol^{-1}

Frontier molecular orbitals analysis

The frontier molecular orbitals (FMOs) are extremely important parameters from quantum chemistry calculations, and their energy gap is a very important description. The FMO analysis of the molecules aids in demonstrating their kinetic stability and chemical reactivity.[63] Chemical hardness is a good index to estimate the chemical stability of compounds. The molecules with a large energy gap are hard, and those with a small energy gap are soft molecules. The softer molecules are more polarizable due to the less energy needed to overcome the energy gap to excite an electron from HOMO to LUMO.[64] The electronic properties of the **HL** ligands and their copper(II) complexes were computed by the B3LYP method with a Def2-TZVP basis set. The higher occupied and lower unoccupied molecular orbitals of these compounds are presented in Figure 11. In all ligands and complexes, the HOMOs are localized mostly around the aryl rings and the LUMOs are distributed around the aryl and heterocycle rings.

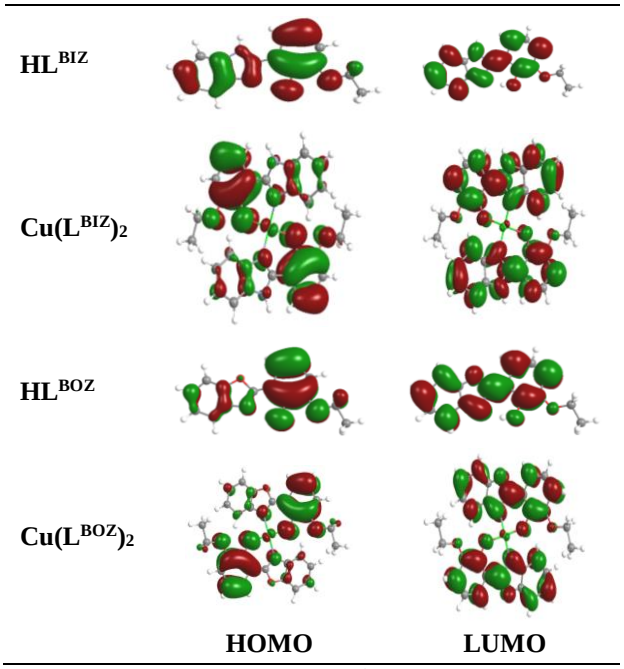

Figure 11. Frontier molecular orbitals of **HL** ligands and their Cu(II) complexes by B3LYP method with Def2-TZVP basis set.

The quantum chemical parameters of the ligands and complexes are listed in Table 6. Based on the results, **Cu(L^{BOZ})$_2$** has the lowest energy gap (3.747 eV) compared to the others, which allows it to be the softest molecule. Therefore, **Cu(L^{BOZ})$_2$** is more reactive than the other complex. The chemical potential values for all the studied compounds are negative and indicate that the compounds are stable and do not decompose into their components.[65,66] In addition, the electrophilicity index values for the complexes show that **Cu(L^{BOZ})$_2$** is a stronger electrophile than the other complex.[67]

Molecular electrostatic potential maps

Molecular electrostatic potential (MEP) is a useful and important parameter for explaining the nucleophilic and electrophilic behavior of molecules. The MEP indicates the size and shape of the molecule as well as the electrostatic region. In MEP, the red, blue, and green colors represent the negative, positive, and neutral electrostatic regions, respectively.[68] To investigate the nucleophilic and electrophilic attack sites of the **HL** ligands and their Cu(II) complexes, MEP was calculated with B3LYP/Def2-TZVP and presented in Figure 12. In the ligands, the most negative regions are around the more electronegative atoms, namely oxygens, sulfur, and

nitrogens, and the most positive regions are around protons. In the complexes, the copper atom located at the center of the positive electrostatic regions represented by the blue color is a good candidate for a nucleophilic attack. Most of the negative charges are located near electronegative atoms, which are attractive sites for protons.

Table 6. Quantum chemical descriptors of the heterocyclic ligands and their copper(II) complexes (in eV)[a]

	HL^{BIZ}	HL^{BOZ}	$Cu(L^{BIZ})_2$	$Cu(L^{BOZ})_2$
E_{HOMO}	-5.938	-6.077	-5.390	-5.561
E_{LUMO}	-1.573	-1.841	-1.507	-1.814
ΔE	4.365	4.236	3.883	3.747
I	5.938	6.077	5.390	5.561
A	1.573	1.841	1.507	1.814
η	2.182	2.118	1.942	1.874
S	0.229	0.236	0.258	0.267
χ	3.756	3.959	3.448	3.688
μ	-3.756	-3.959	-3.448	-3.688
ω	3.232	3.700	3.062	3.628

[a]Energy gap ($\Delta E = E_{LUMO} - E_{HOMO}$); Ionization potential ($I = -E_{HOMO}$); Electron affinity ($A = -E_{LUMO}$); Hardness ($\eta = (I - A)/2$); Softness ($S = 1/2\eta$); Electronegativity ($\chi = (I + A)/2$); Chemical potential ($\mu = -(I + A)/2$); Electrophilicity ($\omega = \mu^2/2\eta$).

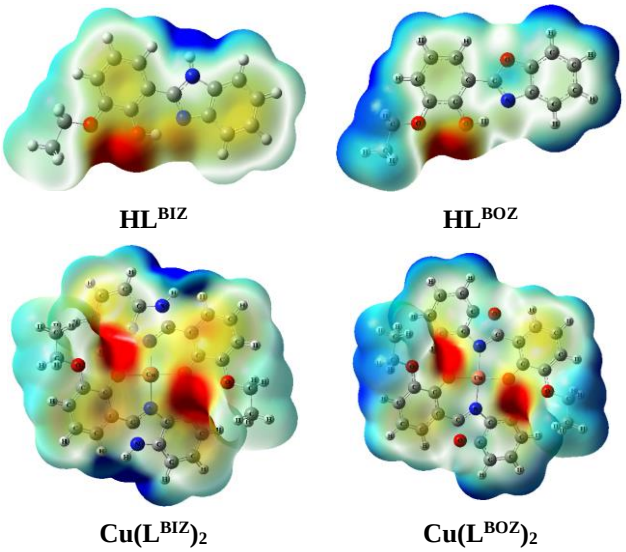

Figure 12. Molecular electrostatic potential maps of the **HL** ligands and their Cu(II) complexes calculated at B3LYP/Def2-TZVP (-0.04 to +0.04 a.u.).

NBO analysis

Natural bond orbital (NBO) analysis is a fundamental tool for studying intermolecular and intramolecular bonding and interactions between donors and acceptors, and it estimates their stabilization energy with second-order perturbations. The NBO also provides an appropriate basis to analyze charge transfer in molecular systems.[69] The NBO analysis for the **$Cu(L^{BIZ})_2$** and **$Cu(L^{BOZ})_2$** complexes was performed using the B3LYP/Def2-TZVP method. The natural charge of the Cu ion (+2.0 e) decreased on complexation (+1.372 and +1.375 e), indicating the electron transfer from the orbitals of oxygen and nitrogen atoms to copper orbitals. The NEC of the free Cu^{2+} ion is $4s^0 3d^9$, whereas the NEC of the Cu ion in the complexes is $4s^{0.29} 3d^{9.31} 4p^{0.01} (4d^{0.01})$. The d-orbital occupancy of the Cu ion in the complexes ($3d^{9.31}$) is higher than that of the free ion ($3d^9$). The s-orbital occupancy of the Cu ion also increased slightly when going from the free ion to the complex. The increase in electron density in the s and d orbitals of the copper ion in the complexes confirms the electron transfer to the central metal (Tables 7 and 8).

The NBO analysis of the **$Cu(L^{BIZ})_2$** and **$Cu(L^{BOZ})_2$** complexes also identified important electron donor and acceptor orbitals. The donor-acceptor orbitals interactions from LP (2) O_1 and LP (1) N_1 to LV (1) Cu_1 in both complexes are presented in Figure 13.

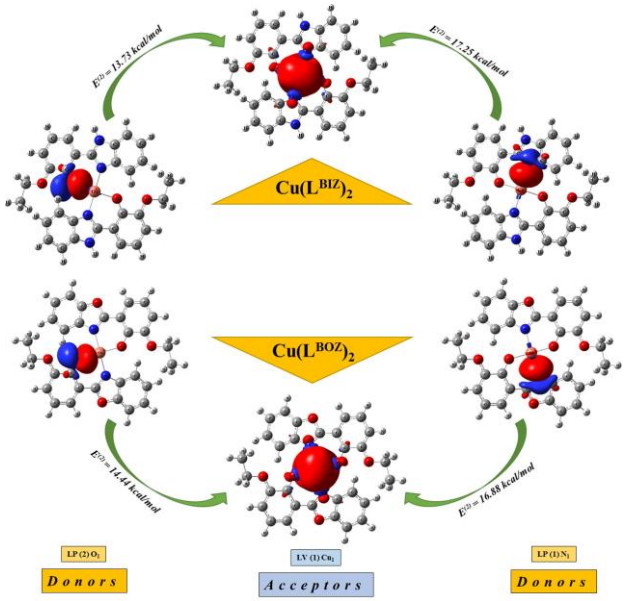

Figure 13. Electron donation from LP (2) O_1 and LP (1) N_1 to LV (1) Cu_1 in **$Cu(L^{BIZ})_2$** and **$Cu(L^{BOZ})_2$** complexes**.**

5.CONCLUSIONS

Heterocyclic ligands under ultrasonic irradiation from the reaction of 3-ethoxy salicylaldehyde with 1,2-phenylenediamine and 2-aminophenol have been successfully designed and synthesized. The synthesis of these ligands was verified to be as forthright as anticipated, generating high yields in simple one-pot condensation reactions. Also, this paper presents the synthesis and characterization of Cu(II) complexes of the heterocyclic ligands. In the bis-chelate copper(II) complexes, the deprotonated heterocyclic ligands formed six-membered rings. According to the results of quantum chemical parameters, **$Cu(L^{BOZ})_2$** has the smallest energy

Table 7. Summary of natural charge, natural population analysis, and natural electronic configuration of **Cu(L^{BIZ})$_2$** by B3LYP method with Def2-TZVP basis set

Atom	Charge	Natural population				Natural electron configuration
		Core	Valence	Rydberg	Total	
Cu_1	1.372	18.000	9.607	0.021	27.628	[core]$4s^{0.29}3d^{9.31}4p^{0.01}$
O_1	-0.773	2.000	6.750	0.023	8.773	[core]$2s^{1.70}2p^{5.05}3p^{0.01}3d^{0.01}$
O_2	-0.452	2.000	6.427	0.025	8.452	[core]$2s^{1.59}2p^{4.84}3p^{0.01}3d^{0.01}$
N_1	-0.571	2.000	5.538	0.033	7.571	[core]$2s^{1.37}2p^{4.17}3p^{0.02}3d^{0.01}$
N_2	-0.502	2.000	5.484	0.018	7.502	[core]$2s^{1.24}2p^{4.25}3p^{0.01}3d^{0.01}$
C_1	0.103	2.000	3.874	0.023	5.897	[core]$2s^{0.88}2p^{3.00}3p^{0.01}$
C_2	-0.194	2.000	4.176	0.017	6.194	[core]$2s^{0.98}2p^{3.20}3p^{0.01}$
C_3	-0.220	2.000	4.203	0.017	6.220	[core]$2s^{0.98}2p^{3.22}3p^{0.01}$
C_4	-0.205	2.000	4.188	0.018	6.205	[core]$2s^{0.98}2p^{3.21}3p^{0.01}$
C_5	-0.242	2.000	4.226	0.017	6.242	[core]$2s^{0.97}2p^{3.26}3p^{0.01}$
C_6	0.107	2.000	3.874	0.019	5.893	[core]$2s^{0.87}2p^{3.00}3p^{0.01}$
C_7	0.419	2.000	3.558	0.023	5.581	[core]$2s^{0.84}2p^{2.72}3p^{0.01}$
C_8	-0.211	2.000	4.193	0.018	6.211	[core]$2s^{0.92}2p^{3.27}3p^{0.01}$
C_9	0.359	2.000	3.613	0.029	5.641	[core]$2s^{0.85}2p^{2.76}3p^{0.01}3d^{0.01}$
C_{10}	0.239	2.000	3.739	0.022	5.761	[core]$2s^{0.88}2p^{2.86}3p^{0.01}$
C_{11}	-0.282	2.000	4.264	0.018	6.282	[core]$2s^{0.98}2p^{3.29}3p^{0.01}$
C_{12}	-0.238	2.000	4.219	0.019	6.238	[core]$2s^{0.96}2p^{3.25}3p^{0.01}$
C_{13}	-0.199	2.000	4.182	0.017	6.199	[core]$2s^{0.96}2p^{3.22}3p^{0.01}$
C_{14}	-0.064	2.000	4.048	0.015	6.064	[core]$2s^{1.03}2p^{3.01}3d^{0.01}$
C_{15}	-0.605	2.000	4.595	0.010	6.605	[core]$2s^{1.12}2p^{3.48}3d^{0.01}$

Table 8. Summary of natural charge, natural population analysis, and natural electronic configuration of **Cu(L^{BOZ})$_2$** by B3LYP method with Def2-TZVP basis set

Atom	Charge	Natural population				Natural electron configuration
		Core	Valence	Rydberg	Total	
Cu_1	1.375	18.000	9.604	0.021	27.625	[core]$4s^{0.29}3d^{9.31}4p^{0.01}4d^{0.01}$
O_1	-0.770	2.000	6.746	0.024	8.770	[core]$2s^{1.70}2p^{5.05}3p^{0.01}3d^{0.01}$
O_2	-0.456	2.000	6.432	0.025	8.456	[core]$2s^{1.59}2p^{4.84}3p^{0.01}3d^{0.01}$
O_3	-0.392	2.000	6.371	0.021	8.392	[core]$2s^{1.60}2p^{4.77}3d^{0.02}$
N_1	-0.582	2.000	5.548	0.034	7.582	[core]$2s^{1.38}2p^{4.17}3p^{0.02}3d^{0.01}$
C_1	0.077	2.000	3.899	0.024	5.923	[core]$2s^{0.88}2p^{3.02}3p^{0.01}$
C_2	-0.194	2.000	4.177	0.017	6.194	[core]$2s^{0.98}2p^{3.20}3p^{0.01}$
C_3	-0.212	2.000	4.195	0.017	6.212	[core]$2s^{0.98}2p^{3.22}3p^{0.01}$
C_4	-0.202	2.000	4.185	0.017	6.202	[core]$2s^{0.98}2p^{3.20}3p^{0.01}$
C_5	-0.246	2.000	4.229	0.017	6.246	[core]$2s^{0.98}2p^{3.25}3p^{0.01}$
C_6	0.237	2.000	3.741	0.022	5.763	[core]$2s^{0.87}2p^{2.87}3p^{0.01}$
C_7	0.553	2.000	3.422	0.025	5.447	[core]$2s^{0.83}2p^{2.59}3p^{0.01}3d^{0.01}$
C_8	-0.233	2.000	4.214	0.019	6.233	[core]$2s^{0.92}2p^{3.29}3p^{0.01}$
C_9	0.365	2.000	3.606	0.028	5.635	[core]$2s^{0.85}2p^{2.75}3p^{0.01}3d^{0.01}$
C_{10}	0.231	2.000	3.746	0.022	5.769	[core]$2s^{0.88}2p^{2.87}3p^{0.01}$
C_{11}	-0.272	2.000	4.254	0.018	6.272	[core]$2s^{0.98}2p^{3.27}3p^{0.01}$
C_{12}	-0.238	2.000	4.220	0.019	6.238	[core]$2s^{0.97}2p^{3.25}3p^{0.01}$
C_{13}	-0.179	2.000	4.162	0.017	6.179	[core]$2s^{0.97}2p^{3.20}3p^{0.01}$
C_{14}	-0.064	2.000	4.049	0.015	6.064	[core]$2s^{1.03}2p^{3.01}3d^{0.01}$
C_{15}	-0.605	2.000	4.595	0.010	6.605	[core]$2s^{1.12}2p^{3.48}3d^{0.01}$

gap (3.747 eV) compared to the other compounds, making it the softest and most reactive molecule among the others. MEP analysis shows that the negative regions are around oxygen and nitrogen, and the most positive regions are around protons. Furthermore, the transfer of electronic density from the filled orbitals of oxygen and nitrogen atoms to the vacant orbitals of the Cu^{+2} ion is indicated by the NBO analysis.

CONFLICTS OF INTEREST

The authors declare that they have no known competing financial interests or personal relationships that could have appeared to influence the work reported in this paper.

ACKNOWLEDGEMENTS

We gratefully acknowledge the practical support for this study by Ardakan University and Payame Noor University.

AUTHOR INFORMATION

Corresponding Author

Hadi Kargar: Emails: h.kargar@ardakan.ac.ir; hadi_kargar@yahoo.com, *ORCID*: 0000-0002-7817-0937

Author(s)

Mehdi Fallah-Mehrjardi, Reza Behjatmanesh-Ardakani, Khurram Shahzad Munawar

REFERENCES

1. N. Mathur, S. Bargotya, *J. Appl. Chem.* **2017**, *10*, 18.
2. N. Mathur, N. Jain, A. K. Sharma, *Open Pharm. Sci. J.* **2018**, *5*, 24.
3. B. G. Cassemiro, J. S. Santos, W. X. Oliveira, E. C. Pereira-Maia, B. R. Galvao, W. D. do Pim, P. P. Silva-Caldeira, *Appl. Organomet. Chem*. **2020**, *34*, e5425.
4. V. Klimesova, J. Koci, K. Waisser, J. Kaustova, *Il Farmaco*, **2002**, 57, 259.
5. N. M. Agh-Atabay, B. Dulger, F. Gucin, *Eur. J. Med. Chem*. **2003**, *38*, 875.
6. A. Tavman, N. M. Agh-Atabay, A. Neshat, F. Gucin, B. Dulger, D. Haciu, *Transition Met. Chem.* **2006**, *31*, 194.
7. A. Khalafi-Nezhad, M. N. Soltani Rad, H. Mohabatkar, Z. Asrari, B. Hemmateenejad, *Bioorg. Med. Chem.* **2005**, *13*, 1931.
8. J. Mann, A. Baron, Y. Opoku-Boahen, E. Johansson, G. Parkinson, L. R. Kelland, S. Neidle, *J. Med. Chem.* **2001**, *44*, 138.
9. J. L. Adams, J. C. Boehm, T. F. Gallagher, S. Kassis, E. F. Webb, R. Hall, M. Sorenson, R. Garigipati, D. E. Griswold, J. C. Lee, *Bioorg. Med. Chem. Lett.* **2001**, *11*, 2867.
10. R.K. Ujjinamatada, A. Baier, P. Borowski, R.S. Hosmane, Bioorg. Med. Chem. Lett. 2007, 17, 2285.
11. S.A.F. Rostom, H.M.A. Ashour, H.A.A.E. Razik, A.E.F.H.A.E. Fattah, N.N. El-Din, *Bioorg. Med. Chem.* **2009**, *17*, 2410.
12. 12. B. Ulkuseven, A. Tavman, G. Otuk, S. Birteksoz, *Folia Microbiol.* **2002**, *47*, 481.
13. N.M. Agh-Atababy, A. Baykal, M. Somer, *Transition Met. Chem.* **2004**, *29*, 159.
14. A. Tavman, B. Ulkuseven, *Main Group Met. Chem.* **2001**, *24*, 205.
15. B. Kumari, S. Adhikari, J.S. Matalobos, D. Das, *J. Mol. Struct.* **2018**, *1151*, 169.
16. J. Zhao, S. Zhi, H. Yu, R. Mao, J. Hu, W. Song, J. Zhang, *RSC Adv.* **2017**, *7*, 51162.
17. Dyukova, L.G. Lavrenova, T.A. Kuzmenko, V.Y. Komarov, T.S. Sukhikh, E.V. Vorontsova, *Inorg. Chim. Acta* **2019**, *486*, 406.
18. B. Shankar, F. Hussain, M. Sathiyendiran, *J. Organomet. Chem.* **2012**, *719*, 26.
19. E. Lukevics, P. Arsenyan, I. Shestakova, I. Domracheva, A. Nesterova, O. Pudova, *Eur. J. Med. Chem.* **2001**, *36*, 507.
20. H. Wu, F. Kou, F. Jia, B. Liu, J. Yuan, Y. Bai, *Bioinorg. Chem. Appl.* **2011**, 105431.
21. J. Hu, C. Liao, R. Mao, J. Zhang, J. Zhao, Z. Gu, *Med. Chem. Comm*. **2018**, *9*, 337.
22. P. Naveen, R. Jain, P. Kalaivani, R. Shankar, F. Dallemer, R. Prabhakaran, *New J. Chem.* **2017**, *41*, 8885.
23. Y.Y. Qi, Q. Gan, Y.X. Liu, Y.H. Xiong, Z.W. Mao, X.Y. Le, *Eur. J. Med. Chem.* **2018**, *154*, 220.
24. X. Wang, N. Ling, Q.T. Che, Y.W. Zhang, H.X. Yang, Y. Ruan, T.T. Zhao, *Inorg. Chem. Commun.* **2019**, *105*, 97.
25. D.F. Back, G.M. de Oliveira, M.A. Ballin, V.A. Corbellini, *Inorg. Chim. Acta* **2010**, *363*, 807.
26. H. Razavi, S.K. Palaninathan, E.T. Powers, R.L. Wiseman, H.E. Purkey, N.N. Mohamedmohaideen, S. Deechongkit, K.P. Chiang, M.T.A. Dendle, J.C. Sacchettini, J.W. Kelly, *Angew. Chem., Int. Ed.* **2003**, *115*, 2864.
27. H. Razavi, S.K. Palaninathan, E.T. Powers, R.L. Wiseman, H.E. Purkey, N.N. Mohamedmohaideen, S. Deechongkit, K.P. Chiang, M.T.A. Dendle, J.C. Sacchettini, J.W. Kelly, *Angew. Chem., Int. Ed.* **2003**, *115*, 2758.
28. J. Koci, V. Klimesova, K. Waisser, J. Kaustova, H.M. Dahse, U. Mollmann, *Bioorg. Med. Chem. Lett.* **2002**, *12*, 3275.
29. D.F. Shi, T.D. Bradshaw, S. Wrigley, C.J. McCall, P. Lelieveld, I. Fichtner, M.F. Stevens, *J. Med. Chem.* **1996**, *39*, 3375.
30. Y. Wu, X. Han, Y. Qu, K. Zhao, C. Wang, G. Huang, H. Wu, *J. Mol. Struct.* **2019**, *1191*, 95.

31. D. Marcinkowski, M. A. Fik, T. Luczak, M. Kubicki, V. Patroniak, *Polyhedron* **2018**, *141*, 125.
32. S. Chacko, H. Boshoff, V. Singh, D. M. Ferraris, D. R. Gollapalli, M. J. Zhang, A. P. Lawson, M. J. Pepi, A. Joachimiak, M. Rizzi, V. Mizrahi, G. D. Cuny, L. Hedstrom, *J. Med. Chem.* **2018**, *61*, 4739.
33. J. Jiang, X. Tang, W. Dou, H. Zhang, W. Liu, C. Wang, J. Zheng, *J. Inorg. Biochem.* 2010, *104*, 583.
34. M. I. Knyazhanskii, P. V. Gilyanovskii, A. E. Lyubarskaya, *Zh. Obshch. Khim.* **1980**, *50*, 2553.
35. G. Spengler, A. Kincses, B. Racz, B. Varga, G. Watanabe, R. Saijo, H. Sekiya, E. Tamai, J. Maki, J. Molnar, M. Kawase, *Anticancer Res.* **2018**, *38*, 6181.
36. A. Sahraei, H. Kargar, M. Hakimi, M. N. Tahir, *J. Mol. Struct.* **2017**, *1149*, 576.
37. A. Sahraei, H. Kargar, M. Hakimi, M. N. Tahir, *Transition Met. Chem.* **2017**, *42*, 483.
38. H. Kargar, V. Torabi, A. Akbari, R. Behjatmanesh-Ardakani, M. N. Tahir, *J. Mol. Struct.* **2019**, *1179*, 732.
39. H. Kargar, V. Torabi, A. Akbari, R. Behjatmanesh-Ardakani, A. Sahraei, M. N. Tahir, *Struct. Chem.* **2019**, *30*, 2289.
40. H. Kargar, A. Adabi Ardakani, K. S. Munawar, M. Ashfaq, M. N. Tahir, *J. Iran. Chem. Soc.* **2021**, *18*, 2493.
41. H. Kargar, R. Behjatmanesh-Ardakani, V. Torabi, M. Kashani, Z. Chavoshpour-Natanzi, Z. Kazemi, V. Mirkhani, A. Sahraei, M. N. Tahir, M. Ashfaq, K. S. Munawar, *Polyhedron* **2021**, *195*, 114988.
42. H. Kargar, R. Behjatmanesh-Ardakani, V. Torabi, A. Sarvian, Z. Kazemi, Z. Chavoshpour-Natanzi, V. Mirkhani, A. Sahraei, M. N. Tahir, M. Ashfaq, K. S. Munawar, *Inorg. Chim. Acta* **2021**, *514*, 120004.
43. H. Kargar, M. Bazrafshan, M. Fallah-Mehrjardi, R. Behjatmanesh-Ardakani, H. Amiri Rudbari, K. S. Munawar, M. Ashfaq, M. N. Tahir, *Polyhedron* **2021**, *202*, 115194.
44. H. Kargar, P. Forootan, M. Fallah-Mehrjardi, R. Behjatmanesh-Ardakani, H. Amiri Rudbari, K.S. Munawar, M. Ashfaq, M. N. Tahir, *Inorg. Chim. Acta* **2021**, *523*, 120414.
45. H. Kargar, M. Fallah-Mehrjardi, R. Behjatmanesh-Ardakani, K. S. Munawar, M. Ashfaq, M. N. Tahir, *J. Mol. Struct.* **2021**, *1241*, 130653.
46. C. S. Yeap, H. Karagr, R. Kia, A. Jamshidvand, H.-K. Fun, *Acta Cryst.* **2009**, *E65*, o745.
47. M. J. Frisch, G. W. Trucks, H. B. Schlegel, G. E. Scuseria, M. A. Robb, J. R. Cheeseman, G. Scalmani, etc. GAUSSIAN 09 (Revision D.01), Gaussian, Inc., C.T. Wallingford (**2013**).
48. A. D. Becke, *J. Chem. Phys.* **1993**, *98*, 5648.
49. J. Tomasi, B. Mennucci, R. Cammi, *Chem. Rev.* **2005**, *105*, 2999.
50. F. Weigend, R. Ahlrichs, *Phys. Chem. Chem. Phys.* **2005**, *7*, 3297.
51. J. Gauss, *J. Chem. Phys.* **1993**, *99*, 3629.
52. http://www.chemissian.com.
53. E. D. Glendening, J. K. Badenhoop, A. E. Reed, J. E. Carpenter, J. A. Bohmann, C. M. Morales, C. R. Landis, F. Weinhold, Theoretical Chemistry Institute, University of Wisconsin, Madison, WI (**2013**).
54. A. Jamshidvand, M. Sahihi, V. Mirkhani, M. Moghadam, I. Mohammadpoor-Baltork, S. Tangestaninejad, H. Amiri Rudbari, H. Kargar, R. Keshavarzi, S. Gharaghani, *J. Mol. Liq.* **2018**, *253*, 61.
55. B. Khera, A. K. Sharma, N. K. Kaushik, *Polyhedron* **1983**, *2*, 1177.
56. G. Gupta, R. Sharan, R. N. Kapoor, *Transition Met. Chem.* **1978**, *3*, 282.
57. J. D. Crane, R. Hughes, E. Sinn, *Inorg. Chim. Acta* **1995**, *237*, 181.
58. M. A. Palafox, *Phys. Sci. Rev.* **2018**, *3*, 1.
59. X. Quezada-Buendia, A. Esparza-Ruiz, A. Pena-Hueso, N. Barba-Behrens, R. Contreras, A. Flores-Parra, S. Bernes, S. E. Castillo-Blum, *Inorg. Chim. Acta* **2008**, *361*, 2759.
60. J. D. Crane, R. Hughes, E. Sinn, *Inorg Chim. Acta* **1995**, *237*, 181.
61. L. Benisvy, E. Bill, A. J. Blake, D. Collison, E. S. Davies, C. D. Garner, G. McArdle, E. J. L. McInnes, J. McMaster, S. H. K. Ross, C. Wilson, *Dalton Trans.* **2006**, 258.
62. F. Z. C. Fellah, J. -P. Costes, C. Duhayon, J. C. Daran, J. -P. Tuchagues, *Polyhedron* **2010**, *29*, 2111.
63. C. Tabares-Mendoza, P. Guadarrama, *J. Organomet. Chem.* **2006**, *691*, 2978.
64. P. Geerlings, F. De Proft, W. Langenaeker, *Chem. Rev.* **2003**, *103*, 1793.
65. V. K. Choudhary, A. K. Bhatt, D. Dash, N. Sharma, *J. Comput. Chem.* **2019**, *40*, 2354.
66. T. T. Adejumo, N. V. Tzouras, L. P. Zorba, D. Radanović, A. Pevec, S. Grubišić, D. Mitić, K. K. Anđelković, G. C. Vougioukalakis, B. Čobeljić, I. Turel, *Molecules* **2020**, *25*, 4043.
67. N. V. Tzouras, S. P. Neofotistos, G. C. Vougioukalakis, *ACS Omega* **2019**, *4*, 10279.
68. Z. Demircioğlu, Ç. Albayrak, O. Büyükgüngör, *J. Mol. Struct.* **2014**, *1065*, 210.
69. L. Wei, Y. She, Y. Yu, X. Yao, S. Zhang, *J. Mol. Model.* **2012**, *18*, 2483.